Virology 531 (2019) 19–30

Contents lists available at ScienceDirect

Virology

journal homepage: www.elsevier.com/locate/virology

A high-throughput screen for genes essential for PRRSV infection using a *piggyBac*-based system

Jianhui Bai[a,1], Kongpan Li[a,1], Wenda Tang[a,1], Zuoxiang Liang[a], Xifeng Wang[b], Wenhai Feng[a], Shujun Zhang[c], Liming Ren[a], Sen Wu[a,*], Haitang Han[a,*], Yaofeng Zhao[a,*]

[a] State Key Laboratory of Agrobiotechnology, College of Biological Sciences, National Engineering Laboratory for Animal Breeding, China Agricultural University, Beijing 100193, PR China
[b] Key Laboratory of Animal Ecology and Conservation Biology, Institute of Zoology, Chinese Academy of Science, Beijing 100101, PR China
[c] Key Laboratory of Agricultural Animal Genetics, Breeding and Reproduction of Ministry of Education, Huazhong Agricultural University, Wuhan, Hubei, PR China

ARTICLE INFO

Keywords:
piggyBac transposon
High-throughput screen
Porcine reproductive and respiratory syndrome virus (PRRSV)
CDK17
RNF168
BCL2L15
TRIM33

ABSTRACT

In this study, using a dual-functional, *piggyBac* transposon-based system, we developed a method to systematically decipher the host genes that may be associated with porcine reproductive and respiratory syndrome virus (PRRSV) infection. A Marc145 cell library, which was randomly mutated by transfecting *piggyBac* plasmids, was challenged with PRRSV. The surviving cell clones were subjected to inverse PCR and high-throughput sequencing to map the integration sites of the transposon. Detailed annotation of the genes flanking the integration sites allowed us to generate a ranked list of candidate genes. Among the predicted genes with a high priority, four genes, *CDK17*, *RNF168*, *BCL2L15*, and *TRIM33*, were strongly correlated with PRRSV infection in both Marc145 cells and porcine primary alveolar macrophages. This study not only assists in identifying the genes essential for PRRSV infection but also confirms the possibility of using the *piggyBac* system to study other virus-host genetic interactions in a high-throughput manner.

1. Introduction

Porcine reproductive and respiratory syndrome (PRRS), which typically manifests as reproductive failure in sows and respiratory disease in growing pigs (Han et al., 2017), is a highly contagious disease and has caused significant economic losses worldwide in recent decades. The causative pathogen of PRRS, porcine reproductive and respiratory syndrome virus (PRRSV), is an enveloped, single-stranded RNA virus that belongs to the genus *Arterivirus*, family *Arteriviridae*, and order *Nidovirales*. Traditional control strategies and vaccines for PRRSV are not sufficient to provide sustainable and efficient protection for pigs, mainly due to the variability and immune evasion of PRRSV (Thanawongnuwech and Suradhat, 2010). However, a lack of understanding of the interactions between PRRSV and its host, as well as the genetic factors associated with PRRSV resistance and susceptibility, limits our ability to prevent PRRSV infection.

In recent years, researchers have conducted many studies to identify novel genes related to PRRSV resistance at the whole-genome level. Some studies on natural genetic differences in the resistance/susceptibility of pigs to PRRS in various swine breeds and populations have provided insights to improve our understanding of PRRSV infection (Lunney and Chen, 2010; Petry et al., 2005; Rowland et al., 2012). However, the phenotypes responsible for resistance to PRRSV infection are usually not consistent across different pig breeds, even across different pig populations (Reiner, 2016), which may lead to poor correlations between candidate genes and resistance phenotypes. Therefore, researchers have begun to search for other robust systems to study the genetic factors that underlie PRRSV resistance/susceptibility at the whole-genome level.

Recently, advances in sequencing and functional genomics have facilitated unbiased genome-wide screening of cellular factors related to viral infection. These screening platforms are mainly based on cultured cell lines. Thus far, newly developed gene-editing technologies have expanded the repertoire of available cell types, which is particularly vital for studying viruses that exhibit relatively narrow cytotropism or species tropism (Ramage and Cherry, 2015). For PRRSV, swine are the only known natural hosts, and porcine primary alveolar macrophages (PAMs) are the primary cell targets in vivo. However, in vitro, only the immortalized African green monkey kidney cell line MA-104 and its derivatives, such as Marc145 cells, are susceptible and

* Corresponding authors.
E-mail addresses: swu@cau.edu.cn (S. Wu), hanhaitang@cau.edu.cn (H. Han), yaofengzhao@cau.edu.cn (Y. Zhao).
[1] These authors contributed equally to this work.

https://doi.org/10.1016/j.virol.2019.03.001
Received 5 December 2018; Received in revised form 2 March 2019; Accepted 2 March 2019
Available online 04 March 2019
0042-6822/

permissive to PRRSV infection (Kim et al., 1993). Hence, the major hurdle to performing genome-wide screens for host genes that participate in PRRSV infection has been the development of a gene-editing method suitable for Marc145 cells.

In recent years, an increasing number of unbiased forward and reverse genetic screening methods, including RNA interference (RNAi), cDNA overexpression, the CRISPR/Cas9 system and transposon mutagenesis, have been used to identify host factors (Ramage and Cherry, 2015). However, some of these methods are not broadly used, such as the RNAi method, which exhibits significant potential for false-positive results due to off-target effects (Hao et al., 2013), and the cDNA method, which induces nonphysiologically high expression levels that are not subjected to endogenous regulatory mechanisms (Xue et al., 2016). Based on the existing evidence, CRISPR screening is generally more reliable and more specific than RNAi. Moreover, CRISPR screening has been applied to various functional genomic studies, such as identifying genes required for cell survival or resistance to drugs or viruses (Kim et al., 2017; Wang et al., 2015; Xue et al., 2016). However, in the case of PRRSV, no ready-made sgRNA library is available for Marc145 cells.

The *piggyBac* (PB) system from the cabbage looper moth has been engineered to be highly active in mammalian cells (Ding et al., 2005). Moreover, the simplicity of the *piggyBac* integration machinery, which enables the integration of long DNA sequences, has facilitated the development of a variety of powerful mutagenesis strategies to perform both forward and reverse genetic screens (Chew et al., 2011; Ivics et al., 2009). First, if transposons are integrated within genes, it is possible to conduct loss-of-function screening at the genome-wide level. Second, the incorporation of functional enhancers induces the overexpression of genes flanking these elements (Walden et al., 1994). Two of the best examples are the use of the *piggyBac* transposon for the discovery of cancer genes (Rad et al., 2010) and pluripotency regulators (Guo et al., 2011). In recent years, the transposon-based method has shown great potential for gene discovery because it can combine the strong screening phenotypes of 'gain of function' and 'loss of function' with the ability to cover the whole genome (Chen et al., 2013). In this case, *piggyBac* transposon genetic screening is superior to other methods with the advantages of simplicity, convenience and low cost.

Here, we report the development of a *piggyBac* transposon-based screening method for the discovery of host factors associated with PRRSV resistance/susceptibility. In this study, four of the predicted candidate genes, *CDK17, RNF168, BCL2L15* and *TRIM33*, were strongly correlated with PRRSV infection in both Marc145 cells and PAMs, which confirms the validity of our system. More importantly, this system can be readily applied to other viruses for the identification of host factors responsible for virus resistance/susceptibility.

2. Materials and methods

2.1. Cells and viruses

Marc145 cells (obtained from Prof. Wenhan Feng's laboratory), a monkey kidney cell line that is highly susceptible and permissive to PRRSV infection, were maintained in DMEM supplemented with 10% fetal bovine serum (FBS) and penicillin/streptomycin. Marc145 cells were transfected with DNA constructs using Lipofectamine 2000 or an electrotransfection kit (Lonza) according to the manufacturer's instructions (optimal program: V-013). The modified porcine alveolar macrophage 3D4/21 cell line (CRL-2843) used in our study was provided by Prof. Hanchun Yang and was shown to be susceptible and permissive to PRRSV (Zhang et al., 2018). The cell line was cultured in RPMI-1640 medium (Gibco) supplemented with 10% FBS and penicillin/streptomycin. All cells were cultured in a humidified incubator with 5% CO_2 at 37 °C. 3D4/21 cells were transfected with DNA constructs using electrotransfection (Lonza) according to the manufacturer's instructions (optimal program: D-032).

Three type 2 PRRSV strains were used. The first strain was CH-1a, which was the first type 2 PRRSV strain isolated in China (GenBank accession No. AY032626). The second strain was WUH3 (GenBank accession No. HM853673.2). The third strain was XH-GD (GenBank accession No. EU624117.1), which exhibits 99.1% nucleotide sequence identity to JXA1 strain and was one of the epidemic HP-PRRSV strains isolated in Guangdong; this strain was a gift from Prof. Guihong Zhang of South China Agricultural University. These PRRSV strains were propagated in Marc145 cells, and viral titers were determined using a doubling dilution assay; the titers were denoted as the 50% cell culture infective dose ($TCID_{50}$)/mL, as determined using the Reed-Muench method (Wang et al., 2011). The titrated viruses were preserved at −80 °C.

2.2. Plasmid construction

The *piggyBac* transposon plasmids used in our study included the transposon plasmid named pFind1 and the transposase plasmid named 4PB. The pFind1 plasmid contains a cytomegalovirus (CMV) enhancer, an RNA splicing donor (SD) and two splice acceptors (SA) in both orientations, and the 4PB plasmid contains a transposase coding sequence driven by the CAG promoter. The pX330 vector was purchased from Addgene. The sgRNAs were designed based on the sequences of exon 1 of each gene, and the paired synthesized oligonucleotides were then annealed and cloned into the pX330 plasmid according to the protocol from the Zhang laboratory (http://www.addgene.org/crispr/zhang/). All constructs were verified by sequencing, and the sequences of the sgRNAs are listed in Table S1. Genes were amplified from green monkey cDNA or porcine cDNA and cloned into the pcDNA3.1 (+) vector (N-terminal Myc tag). The constructs described above were verified by sequencing, and the sequences of the amplification primers are listed in Table S2.

A green monkey *IFNβ1* luciferase reporter plasmid was constructed by cloning the green monkey *IFNβ1* promoter (340 bp upstream of the transcription start site (TSS) of the green monkey *IFNβ1* gene [NCBI Reference Sequence: NC_023653.1]) into the pGL3-Basic vector (Promega). Vectors carrying different mutants of the *IFNβ1* promoter were constructed by deleting different transcription factor binding sites and then separately cloning the sequences into the pGL3-basic vector. A green monkey *TRIM33* luciferase reporter plasmid was constructed by cloning the green monkey *TRIM33* promoter (1929 bp upstream of the TSS of the green monkey *TRIM33* gene [NCBI Reference Sequence: NC_023661.1]) into the pGL3-Basic vector (Promega). The sequence information for the *TRIM33* promoter is shown in Fig. S3. The luciferase reporter assay was performed with the Dual Luciferase Reporter Assay System (Promega) according to the manufacturer's protocol. The pRL-TK vector expressing the Renilla luciferase gene was used as a normalization control.

2.3. Construction, expression and purification of DRACO

Double-stranded RNA activated caspase oligomerizer (DRACO) is a synthetic protein that includes three parts: protein kinase R (PKR 1–181), which can detect dsRNA; apoptotic protease-activating factor 11–97 (Apaf 11-97), which can help to selectively induce apoptosis in cells containing viral dsRNA; and protein transduction domain 4 (PTD-4), which can help to transport proteins into cells (Guo et al., 2015). In short, DRACO can rapidly kill virus-infected cells but does not affect uninfected cells. The DNA elements encoding DRACO were synthesized by General Biosystems (Anhui, China) and cloned into the expression vector pET-28a (+). The recombinant pET-28a-DRACO plasmid was identified by PCR, restriction enzyme digestion and sequencing. Then, the DRACO protein was successfully expressed and purified in vitro.

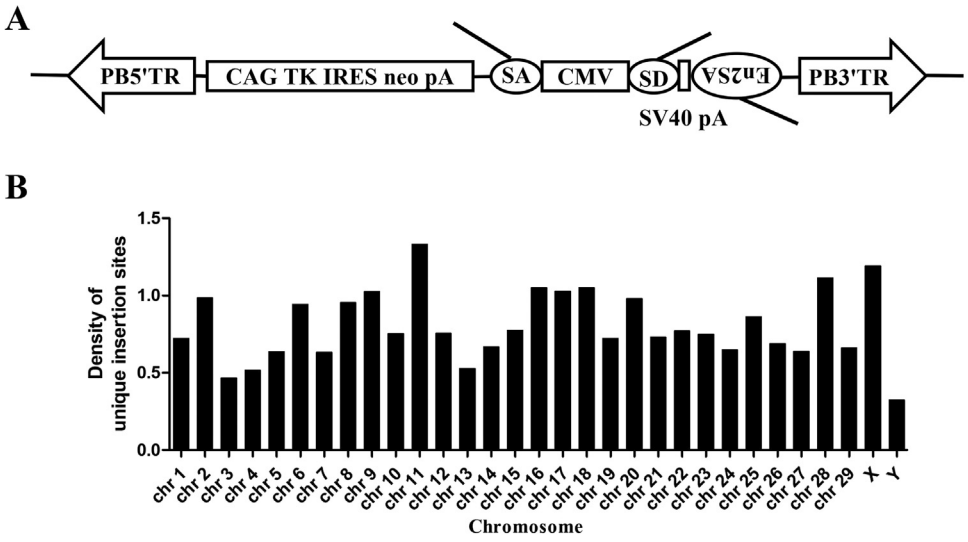

Fig. 1. Generation of the *piggyBac* transposon-mutated library. (A) Diagram of the pFind1 *piggyBac* vector that contains a cytomegalovirus (CMV) enhancer, a neomycin (G418) resistance gene and a gene-trap cassette. SA, splice acceptor; En2SA, splice acceptor in the opposite orientation; SD, splice donor. The 4PB transposase vector contains a transposase coding sequence driven by the CAG promoter. (B) The distribution of unique insertion sites throughout the genome in the mutated cell library. All *piggyBac* insertion sites identified by next-generation sequencing were widely distributed over 31 chromosomes. The X-axis indicates the chromosome. The Y-axis indicates the density of unique insertion sites.

2.4. Quantitative real-time PCR (qRT-PCR)

Total RNA was extracted with TRIzol (Magen) according to the manufacturer's instructions. M-MLV reverse transcriptase was used for reverse transcription according to the manufacturer's protocol (Promega). The qRT-PCR analysis was performed in 96-well plates using the Roche Light Cycler 480 System. The relative expression level of these genes was calculated using the $2^{-\Delta\Delta ct}$ method, and GAPDH mRNA was used as the endogenous control. The primers used for qRT-PCR amplification are listed in Table S2. qRT-PCR was performed on each sample in triplicate.

2.5. Western blotting

Marc145 cells were lysed using immunoprecipitation (IP) lysis buffer containing protease inhibitors (Biotechnology, China). The protein concentrations of the extracts were measured with a BCA assay (Beyotime). Equal amounts of protein from each sample were separated on SDS-PAGE gels and then transferred to polyvinylidene difluoride (PVDF) membranes, which were then blocked with 5% milk in TBST at room temperature for one hour. The PRRSV N protein and Myc-tagged proteins were probed with an N-specific polyclonal IgG antibody produced and characterized in our laboratory (1:500 dilution) and a mouse anti-Myc tag monoclonal IgG antibody (1:1000 dilution, CST), respectively. Then, the membranes were incubated with a goat anti-rabbit IgG secondary antibody (for the N polyclonal antibody, 1:10,000 dilution, Beyotime) or a goat anti-mouse IgG secondary antibody (for the Myc tag monoclonal antibody, 1:10,000 dilution, Beyotime) for one hour at room temperature, followed by washes in TBST. GAPDH was used as the control. Proteins were visualized with chemiluminescence.

2.6. Small interfering RNA (siRNA) assay

The siRNAs and the negative control (NC) were synthesized by GenePharma (Suzhou, China), and the sequences of the siRNAs are provided in Table S1. The cells were transfected with 50 nM siRNA using HiPerFect (Qiagen) for 48 h, as previously described (Zhang et al., 2016); then, the cells were infected with PRRSV at an MOI of 1.0 for 36 h. qRT-PCR was performed to detect the expression levels.

2.7. Immunofluorescence assay

To detect PRRSV infection in Marc145 cells, an immunofluorescence assay (IFA) was performed. The cells were fixed with methanol for 10 min at 4 °C, washed with PBS, and then blocked with 1% bovine albumin V in PBS for 30 min. The cells were then incubated with the anti-PRRSV N protein mAb SDOW17 (1:1000, RTI), followed by washes with PBS. Afterwards, the cells were incubated with Alexa Fluor® 488-conjugated goat anti-mouse IgG (H + L) (1:1000, Beyotime) for 1 h at 37 °C. The expression levels of the N protein were examined using a fluorescence microscope.

2.8. Inverse PCR and next-generation sequencing for the mapping of insertion site

Genomic DNA was extracted from samples using the DNeasy Blood & Tissue Kit (Qiagen). Insertion sites were detected by an adapted inverse PCR protocol. Genomic DNA digested by *Msp* I and *Dpn* I was purified on Qiagen columns and then self-ligated to serve as templates for PCR. We performed one round of inverse PCR to amplify pFind1 insertion sites for sequencing analysis in order to reduce the influence of PCR bias on next-generation sequencing. The amplification primers are PB152 and PB36inv5F, whose sequences are listed in Table S2. The Expand Long Range dNTP Pack (Roche) was used for amplification reactions. The PCR conditions were described in a previously reported protocol (Wu et al., 2007). The amplified PCR products were sent to a sequencing company (Tang Tang Tian Xia, Beijing). The sequencing results were analyzed with Ensembl BLAST.

2.9. Statistical analysis

Generally, all experiments were performed with at least three independent replicates and with three technical replicates per sample. GraphPad Prism software (GraphPad, San Diego, CA) was used to analyze the data. Differences were analyzed using Student's *t*-test, and the results are presented as the mean ± SEM (*$p < 0.05$, **$p < 0.01$, and ***$p < 0.001$).

3. Results

3.1. Generation of a mutated Marc145 cell library using a piggyBac transposon-based system

The modified *piggyBac* transposon system used in our study contains a transposon plasmid named pFind1 and a transposase plasmid named 4PB. The pFind1 plasmid contains a cytomegalovirus (CMV) enhancer, an RNA SD and two SAs in both orientations (Fig. 1**A**). The transposon-based system is thus bifunctional. It causes a loss of gene function when the transposon is directly inserted within genes, regardless of the orientation. On the other hand, this system contains a strong enhancer,

which can lead to the overexpression of genes when the transposon is inserted into flanking or intergenic regions. The 4PB plasmid contains a transposase coding sequence driven by the CAG promoter that can mediate the transposition process by recognizing inverted terminal repeats.

To construct a mutated Marc145 cell library, approximately 5×10^7 cells were cotransfected with the pFind1 and 4PB plasmids by electroporation. Then, the cells were treated with neomycin (G418) and cultured for an additional 10–14 days. Cells that survived the G418 treatment were harvested and cryopreserved as the transposon-mutated library.

To determine the genomic distribution of transposon insertion sites in the mutated library, the genomic DNA isolated from the mutated library was subjected to inverse PCR to amplify the segments flanking the insertion sites. Then, the flanking segments (read number ≥ 3) were mapped to the reference genome, and the insertion sites were characterized for their distribution throughout the genome (Table S3). The density of insertion was then presented based on the ratio of the number of unique insertion sites to the genomic size of each chromosome (Fig. 1**B**). The insertion sites were mapped to all 31 chromosomes, revealing broad coverage throughout the genome. In addition, the density of unique insertion sites (insertion sites per Mb) ranged from 0.32 to 1.33, suggesting that the insertion sites in the mutated cell library exhibited a relatively even distribution throughout the genome.

3.2. Generation of a PRRSV-resistant cell library

To generate a PRRSV-resistant cell library, the mutated cell library and wild-type Marc145 cells that served as the NC, were infected with the CH-1a/WUH3/XH-GD PRRSV strains (Fig. 2**A**). These three strains were used for two major reasons. First, these strains grow stably and robustly under laboratory conditions. Second, CH-1a PRRSV represents a traditional strain, and WUH3/XH-GD PRRSV represent highly pathogenic PRRSV (HP-PRRSV) strains, enabling us to enrich cells that are potentially resistant to several PRRSV strains. After conducting titration to identify the MOI that caused the strongest cytopathic effect (CPE), an MOI of 10 was observed to be the optimal dose. However, we found that not all of the wild-type Marc145 cells died following PRRSV infection (Fig. S1), although a high MOI (MOI = 10) of PRRSV was theoretically sufficient to infect all wild-type Marc145 cells.

To remove the population of PRRSV-infected cells that were not dead, we employed the DRACO protein in our experiments (Fig. S2A), as DRACO has been reported to exert an apoptosis-inducing effect on virus-infected cells when added to the cell supernatant (Guo et al., 2015). As shown in Fig. S2B, the DRACO protein was successfully expressed and purified. Then, the cytotoxicity of the DRACO protein for wild-type Marc145 cells was measured. The results showed that the viability of cells incubated in medium containing 40, 60, or 80 mg/L DRACO protein remained almost normal after treatment for 48 h (Fig. S2C), which was consistent with the reported data (Guo et al., 2015). Then, the function of the DRACO protein was detected using an FITC Annexin V Apoptosis Detection Kit. The results showed that a significantly greater number of apoptotic cells was detected in the DRACO-treated group than in the DRACO-untreated group (Fig. 2**B** and Fig. S2E), indicating that the DRACO protein indeed exerted an apoptosis-inducing effect on PRRSV-infected cells without harming uninfected cells (Fig. S2D). Thus, we added the DRACO protein to the supernatant of cells that had been subjected to several rounds of infections with the three PRRSV strains to clear the surviving PRRSV-infected cells (Fig. 2**A**). As expected, no healthy wild-type Marc145 cells survived, while some healthy cell clones were visible and exhibited a good morphology in the mutated cell library (Fig. 2**C**), indicating that under

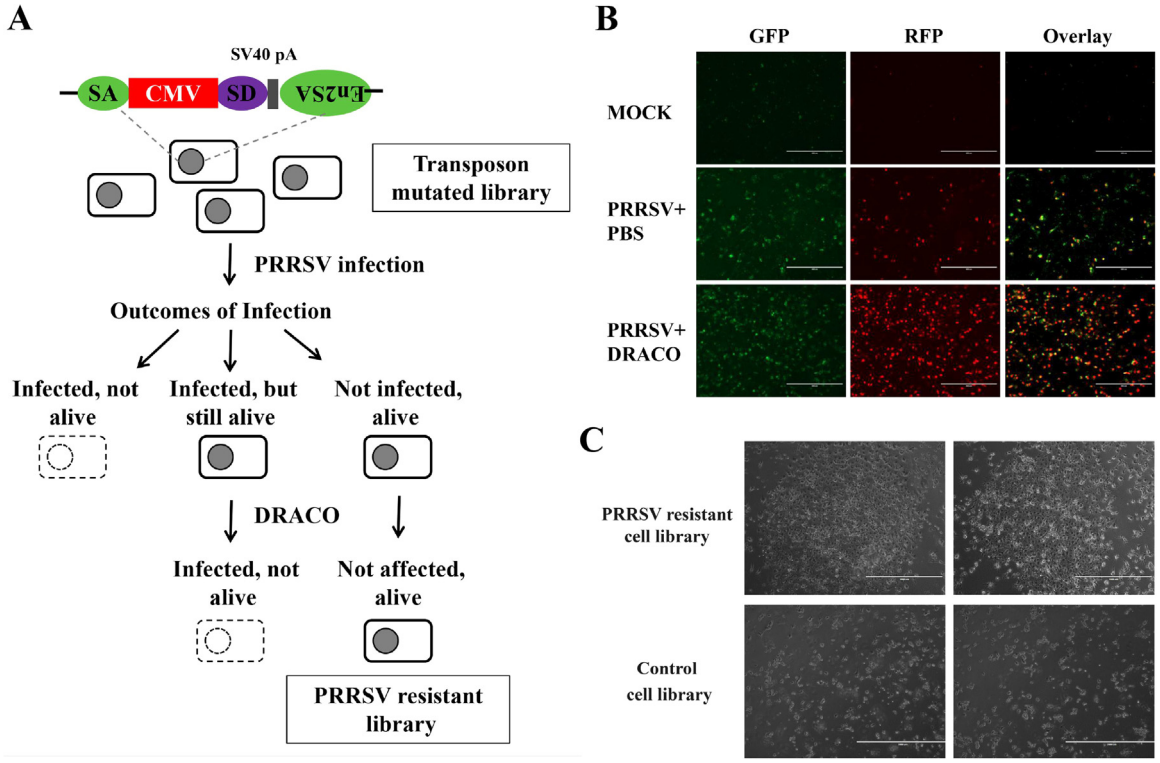

Fig. 2. Generation of the PRRSV-resistant cell library. (A) The process used to screen the PRRSV-resistant cell library. The mutant library was generated by transfecting cells with the *piggyBac* transposon and transposase. Following PRRSV infection and treatment with the DRACO protein, a PRRSV-resistant library was successfully generated. (B) DRACO promoted the apoptosis of PRRSV-infected cells. Cells were infected with CH-1a PRRSV at an MOI of 1.0 in the presence of PBS or DRACO (80 mg/L). The cells were collected at 36 hpi and detected using an FITC Annexin V Apoptosis Detection Kit I. The green color represents early apoptotic cells and the red color represents late apoptotic cells. (C) Images of PRRSV-resistant cells and wild-type control cells after PRRSV infection (For interpretation of the references to color in this figure legend, the reader is referred to the web version of this article).

these conditions, the healthy colonies were likely genetically resistant cell clones arising from transposon insertions.

3.3. List of candidate genes associated with PRRSV resistance/susceptibility

To determine whether PRRSV infection led to an enrichment of transposons at particular insertion sites in the PRRSV-resistant library, the genomic distribution of insertion sites was mapped using inverse PCR and next-generation sequencing analysis. Then, the flanking segments (read number ≥ 3) were mapped to the reference genome, and the insertion sites were also characterized for their distribution throughout the genome (Table S4). The density of insertions was presented based on the ratio of the number of unique insertion sites to the genomic size of each chromosome. The results showed that there were significantly fewer unique insertion sites in the PRRSV-resistant cell library than in the original cell library. Moreover, the maximum read number (2180) for a single insertion site in the PRRSV-resistant cell library was higher than that (844) in the original cell library. In addition, 26 unique insertion sites with read numbers of more than 1000 existed in the PRRSV-resistant cell library. Therefore, a remarkable enrichment of insertion sites was shown in the PRRSV-resistant mutated library compared with the original mutated library (Fig. 3).

To obtain a global perspective of the genes related to PRRSV resistance or susceptibility, these genes were ranked by calculating the pFind1 insertion frequency around each gene (from 200 kb upstream to 200 kb downstream of each gene). The results are presented in Table S5. Subsequently, the ranked genes that were not expressed in PAMs or Marc145 cells were excluded, and those genes with read numbers ≥ 500 are presented in Table S6. To generate a more reasonable candidate gene list for further validation in the follow-up study, we performed a transcriptome analysis of Marc145 cells challenged with CH-1a PRRSV infection, and the results are presented in Table S7. Thus, four genes, *CDK17*, *RNF168*, *BCL2L15* and *HIPK1*, all of which showed significant differential expression after CH-1a PRRSV infection, were chosen as candidate genes for further verification. Because genes related to PRRSV resistance or susceptibility might not always show significant differences in expression after PRRSV infection, four additional genes, *TRIM33*, *ELK3*, *TFRC* and *WDR53*, which are known to be involved in immune responses and stimulus-induced responses, were also chosen for the follow-up study. The final candidate gene list is presented in Table 1.

3.4. Validation of the correlations between candidate genes and PRRSV resistance/susceptibility in Marc145 cells

To verify the correlations between the candidate genes and PRRSV

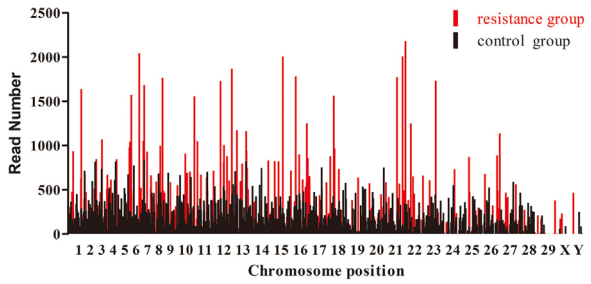

Fig. 3. Characterization of the distribution of insertion sites in the PRRSV-resistant cell library. All *piggyBac* insertion sites in the PRRSV-resistant library were identified by next-generation sequencing. Insertion sites in the PRRSV-resistant library showed a remarkable enrichment compared with the original library. The X-axis indicates the chromosome positions of insertion sites. The Y-axis indicates the raw read number for each site. Red represents the resistance group; black represents the control group (For interpretation of the references to color in this figure legend, the reader is referred to the web version of this article).

Table 1
Candidate gene list.

Gene ID	Gene Name	Ranking	Chromosome location
ENSCSAG00000003573	*ELK3*	7	chr 11
ENSCSAG00000008616	*WDR53*	28	chr 15
ENSCSAG00000001649	*TRIM33*	33	chr 20
ENSCSAG00000008546	*TFRC*	421	chr 15
ENSCSAG00000003570	*CDK17*	8	chr 11
ENSCSAG00000008602	*RNF168*	30	chr 15
ENSCSAG00000001637	*BCL2L15*	351	chr 20
ENSCSAG00000001645	*HIPK1*	348	chr 20

resistance/susceptibility, plasmids containing the candidate genes fused with a Myc tag were constructed and then transfected into Marc145 cells. Western blotting results revealed the overexpression of the eight candidate genes in Marc145 cells (Fig. 4**A**). These cells were then infected with CH-1a PRRSV, and the viral mRNA was detected at 36 h post infection. According to the qRT-PCR results, four genes, *TRIM33*, *CDK17*, *RNF168* and *BCL2L15*, significantly inhibited or enhanced viral infection when overexpressed (Fig. 4**B**).

To further assess these correlations, we individually knocked out *CDK17*, *RNF168*, and *TRIM33* in Marc145 cells. Two independent clonal cell lines were generated for each gene, and the RNA levels of *CDK17*, *RNF168*, and *TRIM33* in the respective knockout cells were determined using RT-PCR and qRT-PCR (Fig. S4). For the *BCL2L15* gene, the knockdown data are presented in Fig. S5A. The results showed a significant decrease in the expression of these genes in the respective knockout or knockdown cells compared with that in the wild-type cells. Next, the cells were collected at the indicated time points after PRRSV infection and examined by qRT-PCR with specific primers for the ORF7 gene. The results showed elevated levels of PRRSV ORF7 mRNA in *CDK17*-knockout cells, *RNF168*-knockout cells, and *BCL2L15*-knockdown cells and reduced levels of PRRSV ORF7 mRNA in *TRIM33*-knockout cells, indicating that CDK17, RNF168, and BCL2L15 inhibited PRRSV infection, while TRIM33 promoted PRRSV infection (Fig. 5A and Fig. S5B). Similar results were obtained for the PRRSV N protein using Western blotting (Fig. 5**B**). Thus, CDK17, RNF168, and BCL2L15 inhibit PRRSV infection, and TRIM33 promotes PRRSV infection, which further confirm the correlation of these four candidate genes with PRRSV infection.

To investigate whether the effects of CDK17, RNF168, BCL2L15 and TRIM33 on PRRSV infection could be replicated in other PRRSV strains in addition to the traditional CH-1a PRRSV strain used above, two highly pathogenic PRRSV strains, WUH3 and XH-GD PRRSV, were utilized to conduct similar experiments. The effects of gene knockout/overexpression (knockdown/overexpression for BCL2L15) on WUH3 and XH-GD PRRSV were consistent with their effects on CH-1a PRRSV, suggesting that the associations of CDK17, RNF168, BCL2L15, and TRIM33 with PRRSV resistance/susceptibility were not restricted to a particular PRRSV strain (Fig. 5**C and** Fig. S5C).

3.5. Validation of the correlations between candidate genes and PRRSV resistance/susceptibility in modified 3D4/21 cells

Because Marc145 cells are not the natural hosts for PRRSV, modified 3D4/21 cells were used to further verify the associations between candidate genes and PRRSV resistance/susceptibility. First, we verified the knockdown efficiency of pTRIM33, pCDK17, pRNF168, and pBCL2L15 in 3D4/21 cells by qRT-PCR after the cells were treated with siRNAs targeting the *TRIM33*, *CDK17*, *RNF168*, and *BCL2L15* genes, respectively, or the NC. The expression of *TRIM33*, *CDK17*, *RNF168* and *BCL2L15* was partially silenced by the respective siRNAs (Fig. 6**A**). Then, the siRNA-transfected cells were infected with WUH3 PRRSV (MOI = 1.0), and the results showed significant changes in PRRSV N mRNA levels, revealing that CDK17, RNF168 and BCL2L15 inhibited

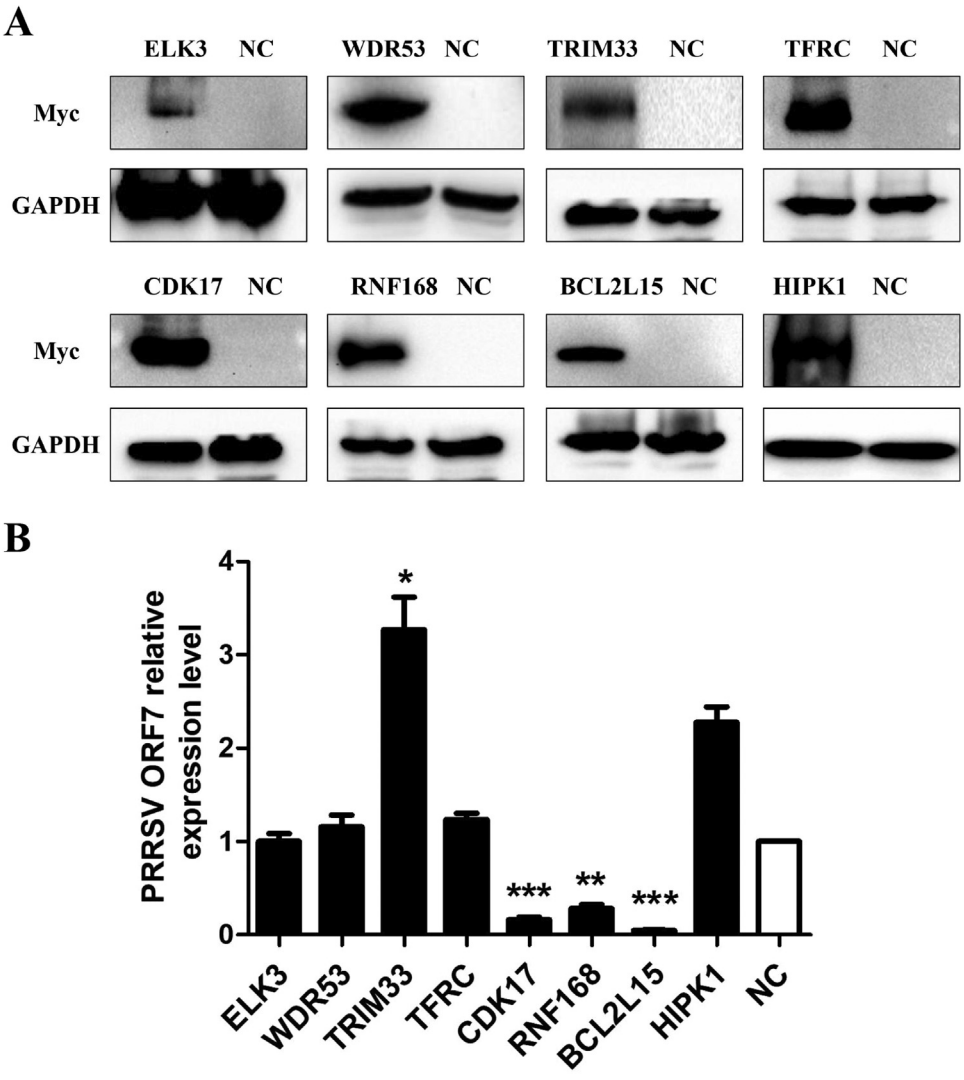

Fig. 4. Preliminary identification of candidate genes. (A) Ectopic expression of eight candidate genes in Marc145 cells. First, Marc145 cells were transfected with vectors expressing Myc-tagged genes and empty vector as the NC for 48 h and then infected with CH-1a PRRSV for another 36 h. The expression of candidate genes was detected with a mouse anti-Myc mAb. GAPDH was detected as an internal control using a mouse anti-GAPDH mAb. (B) qRT-PCR analysis of the viral ORF7 mRNA in candidate gene-overexpressing cells infected with CH-1a PRRSV at 36 hpi. All data are representative of at least three independent experiments. The results are presented as the mean ± SEM (*$p < 0.05$, **$p < 0.01$, and ***$p < 0.001$).

PRRSV infection and that TRIM33 enhanced PRRSV infection in 3D4/21 cells (Fig. 6**B**).

For further validation, these four candidate genes were fused with a Myc tag and overexpressed in the modified 3D4/21 cells. Western blotting results revealed the overexpression of the four candidate genes in 3D4/21 cells (Fig. 6**C**). These cells were then infected with PRRSV, and the viral mRNA was detected at 36 h post infection. According to the qRT-PCR results, four genes, *TRIM33*, *CDK17*, *RNF168* and *BCL2L15*, significantly inhibited or enhanced viral infection when overexpressed in 3D4/21 cells (Fig. 6**D**). Based on these results, TRIM33, CDK17, RNF168 and BCL2L15 were also closely associated with PRRSV resistance/susceptibility in 3D4/21 cells, which was consistent with the findings obtained in Marc145 cells.

3.6. *TRIM33* enhances PRRSV infection

Given that TRIM33 belongs to the TRIM family, which has been implicated in a variety of cellular functions, including antiviral activity, and little is known about how TRIM33 responds to virus infection, the mechanism that underlies the interaction between TRIM33 and PRRSV infection was of interest. To further explain the link between TRIM33 and PRRSV resistance/susceptibility, we investigated whether TRIM33 was regulated by PRRSV infection. A time-course assay was performed to assess the expression of TRIM33 in Marc145 cells infected with the CH-1a PRRSV strain at an MOI of 0.1. Cell samples were collected at 0 hpi, 12 hpi, 24 hpi, 36 hpi, 48 hpi, 60 hpi, and 72 hpi. Then, the *TRIM33* and PRRSV ORF7 mRNA levels of the cell samples collected at each indicated time point were analyzed by qRT-PCR. Our results revealed significantly increased expression of TRIM33 following PRRSV infection (Fig. 7**A left**), and a similar trend was observed for the PRRSV ORF7 mRNA level (Fig. 7**A right**), suggesting that the increase in TRIM33 expression depended on PRRSV infection. To validate the upregulation of TRIM33 by PRRSV infection, the *TRIM33* promoter was transfected into Marc145 cells, and the cells were then infected with CH-1a PRRSV at different MOIs. The results showed that the activity of the promoter was enhanced by PRRSV infection in a dose-dependent manner (Fig. 7**B**).

To further verify the effect of TRIM33 on PRRSV infection, an IFA was also performed in *TRIM33*-knockout cells and wild-type cells after PRRSV infection. The levels of the PRRSV N protein were significantly decreased in *TRIM33*-knockout cells (Fig. 7**C**), which was consistent with the Western blotting data (Fig. 7**D**). To determine the effects of TRIM33 on multicycle PRRSV growth, culture supernatants were collected at the indicated time points to quantify virus yields. As expected, during the late phase of infection, the amount of infectious virus in *TRIM33*-knockout cells was significantly decreased (Fig. 7**E**), indicating that the depletion of TRIM33 markedly inhibited the late phase of PRRSV infection. To exclude a polar effect on *TRIM33*-knockout cells and clearly verify the effect of TRIM33 on PRRSV infection, TRIM33 expression was restored in *TRIM33*-knockout clonal cell lines, which

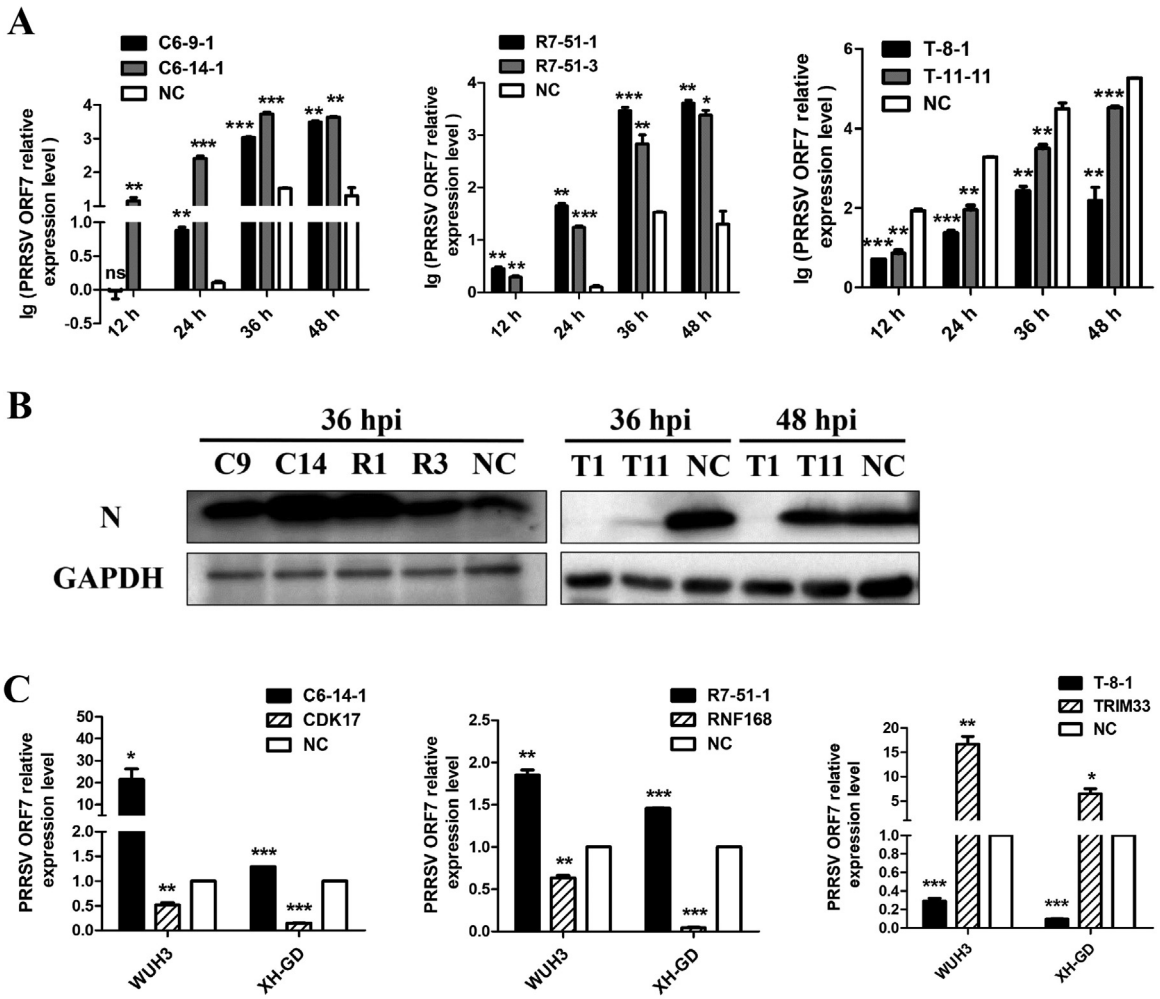

Fig. 5. Validation of correlations between candidate genes and PRRSV resistance/susceptibility in Marc145 cells. (A) Relative levels of PRRSV ORF7 mRNA in *CDK17*-knockout cells (C6-9–1 and C6-14–1), *RNF168*-knockout cells (R7-51–1 and R7-51–3) and *TRIM33*-knockout cells (T-8–1 and T-11–11) versus wild-type Marc145 cells following CH-1a PRRSV infection for 12 h, 24 h, 36 h, 48 h at an MOI of 1.0. The legend of the Y-axis is indicated as lg (PRRSV ORF7 relative expression level). (B) The levels of PRRSV N protein at 36 hpi and/or 48 hpi were examined using Western blotting. C9 and C14 represent two independent *CDK17*-knockout cell clones. R1 and R3 represent two independent *RNF168*-knockout cell clones. T1 and T11 represent two independent *TRIM33*-knockout cell clones. (C) The effects of CDK17, RNF168 and TRIM33 on PRRSV infection were not restricted to a particular PRRSV strain. qRT-PCR analysis of the viral ORF7 mRNA in *CDK17*-knockout cells (C6-14–1), CDK17-overexpressing cells, *RNF168*-knockout cells (R7-51–1), RNF168-overexpressing cells, *TRIM33*-knockout cells (T-8–1), and TRIM33-overexpressing cells after WUH3 and XH-GD PRRSV infection for 36 hpi (normalized to GAPDH). All data are representative of at least three independent experiments. The results are presented as the mean ± SEM (*p < 0.05, **p < 0.01, and ***p < 0.001); ns, not statistically significant.

were subjected to PRRSV infection. The levels of PRRSV ORF7 mRNA in the *TRIM33*-knockout cells increased to a level nearly identical to that observed in wild-type cells (Fig. 7**F**). Thus, TRIM33 indeed facilitated PRRSV infection.

3.7. TRIM33 inhibits IFNβ1 production and signaling primarily by affecting the NF-κB pathway

To investigate the mechanism underlying the TRIM33-induced enhancement of PRRSV infection, we examined whether TRIM33 could alter IFNβ1 production and signaling. First, a qRT-PCR assay was performed to monitor the level of *IFNβ1* mRNA after stimulation with poly (I:C). As expected, the level of *IFNβ1* mRNA was decreased in TRIM33-overexpressing cells but increased in *TRIM33*-knockout cells (Fig. 8**A**). Moreover, a luciferase assay was performed to monitor the activation of the *IFNβ1* promoter after stimulation with poly(I:C), indicating that TRIM33 inhibited the activation of the *IFNβ1* promoter (Fig. 8**B**). These results suggested that TRIM33 impaired IFNβ1 production, verifying the role of TRIM33 as a negative regulator of IFNβ1 production.

As IFN-I activates the JAK-STAT signaling pathway to induce the production of hundreds of interferon-stimulated genes (ISGs) to inhibit viral infection, we performed qRT-PCR to examine the mRNA levels of several important ISGs. The results showed that the expression of *IFIT1*, *IFIT2*, *MX2*, *OAS1* and *OAS3* was increased in *TRIM33*-knockout cells (Fig. 8**C**). Taken together, these results indicated that TRIM33 inhibited IFNβ1 production and signaling.

To further determine the specific region of the *IFNβ1* promoter involved in TRIM33-mediated inhibition of IFNβ1 production, several vectors carrying mutations in the *IFNβ1* promoter were constructed by deleting different transcription factor binding sites and then transfected into *TRIM33*-knockout cells and wild-type cells to analyze transcriptional activity. Our results showed that the activity of the promoter containing the NF-κB-responsive region in *TRIM33*-knockout cells was significantly increased compared with that in wild-type cells, indicating alterations consistent with the *IFNβ1* promoter (Fig. 8**D**). Hence, we speculated that TRIM33 inhibited IFNβ1 production primarily by affecting the NF-κB pathway.

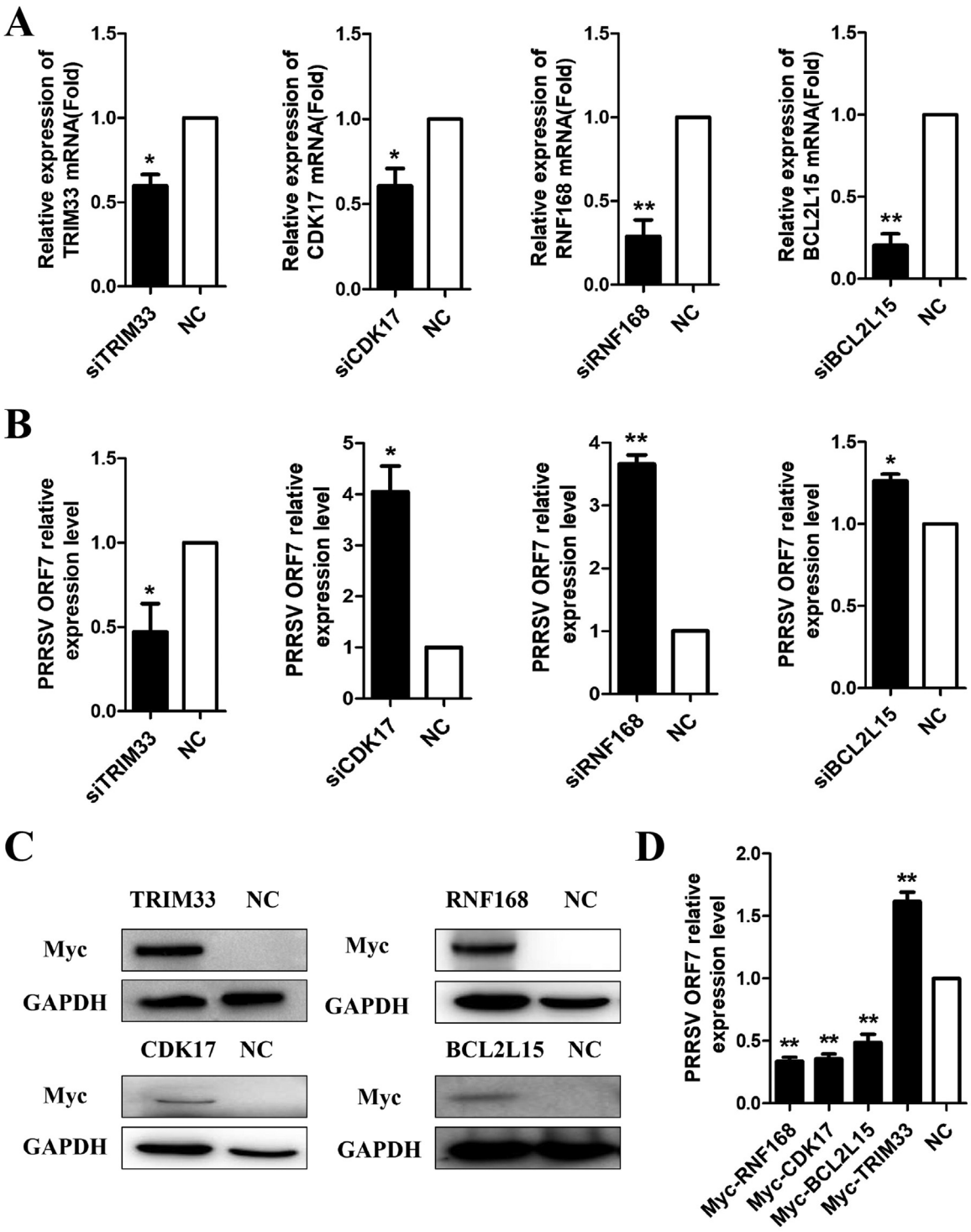

Fig. 6. Validation of correlations between candidate genes and PRRSV infection in 3D4/21 cells. (A) Silencing efficiency of *TRIM33*, *CDK17*, *RNF168* and *BCL2L15* with the respective siRNAs at a final concentration of 50 nM. The expression levels of TRIM33, CDK17, RNF168 and BCL2L15 were examined at 48 h post transfection using qRT-PCR. (B) Relative levels of PRRSV ORF7 mRNA in *TRIM33*, *CDK17*, *RNF168* and *BCL2L15* gene-silenced 3D4/21 cells after WUH3 PRRSV infection. (C) Ectopic expression of four candidate genes in 3D4/21 cells. 3D4/21 cells were electrotransfected with vectors expressing Myc-tagged genes and empty vector as the NC for 48 h and then infected with WUH3 PRRSV for another 36 h. The expression of candidate genes was detected with a mouse anti-Myc mAb. (D) qRT-PCR analysis of the viral ORF7 mRNA in candidate gene-overexpressing cells infected with WUH3 PRRSV at 36 hpi. GAPDH was detected as an internal control using a mouse anti-GAPDH mAb. All data are representative of at least three independent experiments. The results are presented as the mean ± SEM (*$p < 0.05$, **$p < 0.01$, and ***$p < 0.001$).

4. Discussion

This study has reported a genome-wide screening method for the identification of host genes essential for PRRSV infection using the *piggyBac* transposon system and next-generation sequencing technology. A ranked list of host factors potentially associated with PRRSV resistance/susceptibility was generated, among which four major host factors, *CDK17*, *RNF168*, *BCL2L15* and *TRIM33*, were clearly involved

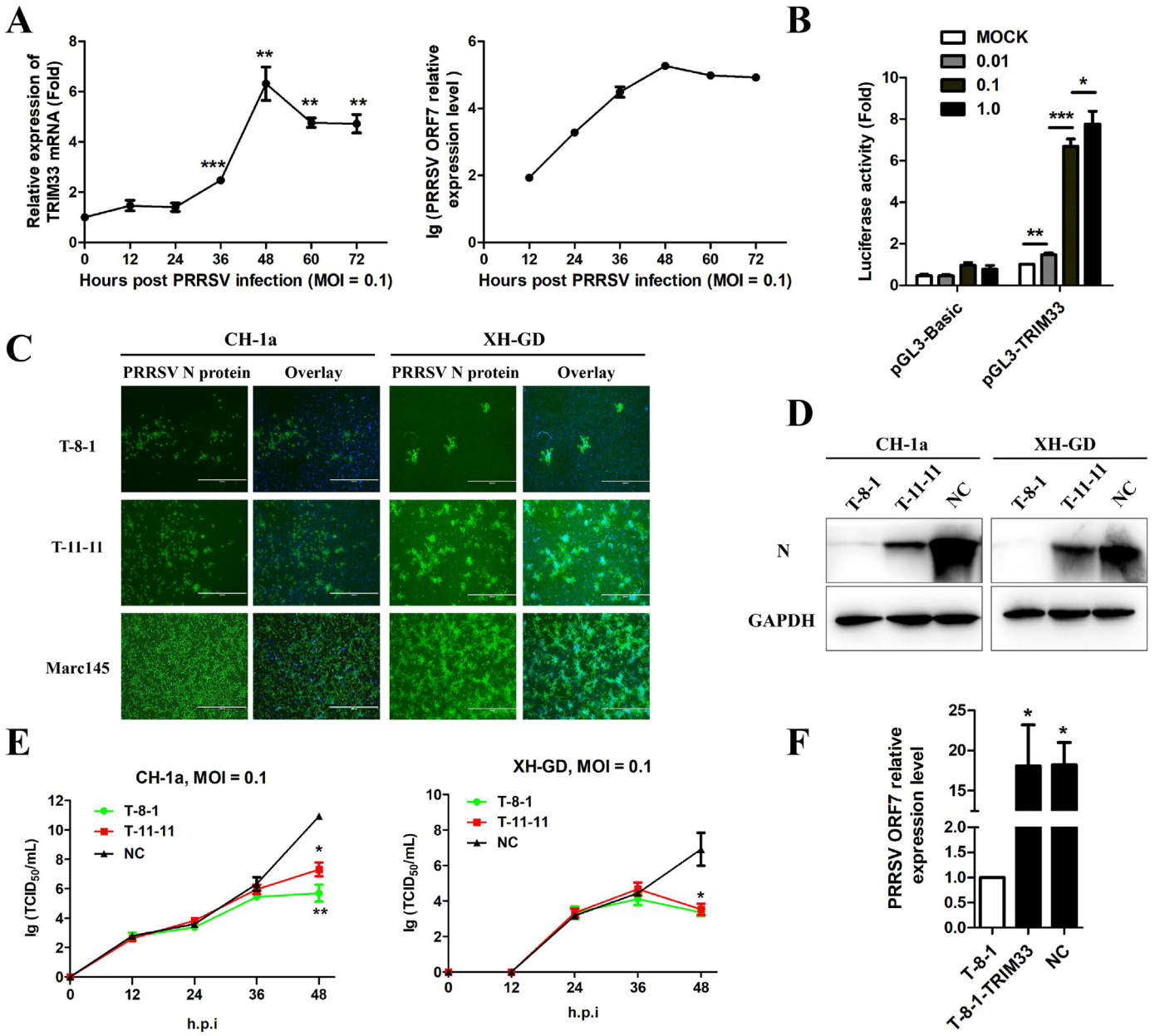

Fig. 7. TRIM33 enhances PRRSV infection. (A) TRIM33 was upregulated by PRRSV. qRT-PCR analysis of the *TRIM33* and PRRSV ORF7 mRNA levels in Marc145 cells infected with CH-1a PRRSV at an MOI of 0.1 for the indicated times. The legend of the Y-axis of the right diagram is indicated as lg (PRRSV ORF7 relative expression level). (B) Marc145 cells were cotransfected with 1 μg of pGL3-basic or pGL3-TRIM33-promoter along with pRL-TK (20 ng) for 6 h and then infected with CH-1a PRRSV at MOIs of 0.01, 0.1 and 1.0. At 48 hpi, luciferase activities were analyzed. (C) *TRIM33*-knockout Marc145 cells (T-8–1 and T-11–11) and wild-type cells were infected with CH-1a and XH-GD PRRSV strains at an MOI of 1.0 for the indicated time points. The cells were fixed for immunofluorescence staining of the PRRSV N protein at 36 hpi. (D) Cells were collected for Western blotting at 36 hpi. (E) The PRRSV titers from the supernatants of infected wild-type Marc145 cells and *TRIM33*-knockout cells (T-8–1 and T-11–11) at 12 hpi, 24 hpi, 36 hpi, 48 hpi, as determined with the $TCID_{50}$ assay. (F) The ectopic expression of TRIM33 protein restores the inhibition of PRRSV infection in *TRIM33*-knockout cells (T-8–1). qRT-PCR analysis of the viral ORF7 mRNA in *TRIM33*-knockout cells transfected with or without Myc-TRIM33 and wild-type Marc145 cells following CH-1a PRRSV infection at 36 hpi (normalized to GAPDH). All data are representative of at least three independent experiments. The results are presented as the mean ± SEM (*$p < 0.05$, **$p < 0.01$, and ***$p < 0.001$).

in the PRRSV infection process. These results confirm the validity of our screening method for the identification of PRRSV infection-associated genes.

As a forward genetic approach, *piggyBac* transposon mutagenesis has been shown to efficiently transpose mammalian cells (YUSA, 2017). These transpositions occur simply based on the *piggyBac* transposon and transposase, whose target site is the TTAA motif, which is fairly abundant in the genome. As reported in previous transposon screens, *piggyBac* transposon-mutated chromosomes are distributed evenly in proportion to their TTAA content (Friedel et al., 2013). Thus, the transpositions mediated by the *piggyBac* transposon do not require a priori knowledge of genetic elements, leading to unbiased mutagenesis throughout the genome.

As the *piggyBac* transposon itself undergoes random insertions throughout the genome, the screening platform based on the *piggyBac* transposon does not require time-consuming procedures to design gene target sites. On the other hand, as stated above, the TTAA motif is extremely common and widespread in the genomes of most species, indicating that a *piggyBac* transposon-based system is readily applicable to new cell lines that are susceptible and permissive to other viruses.

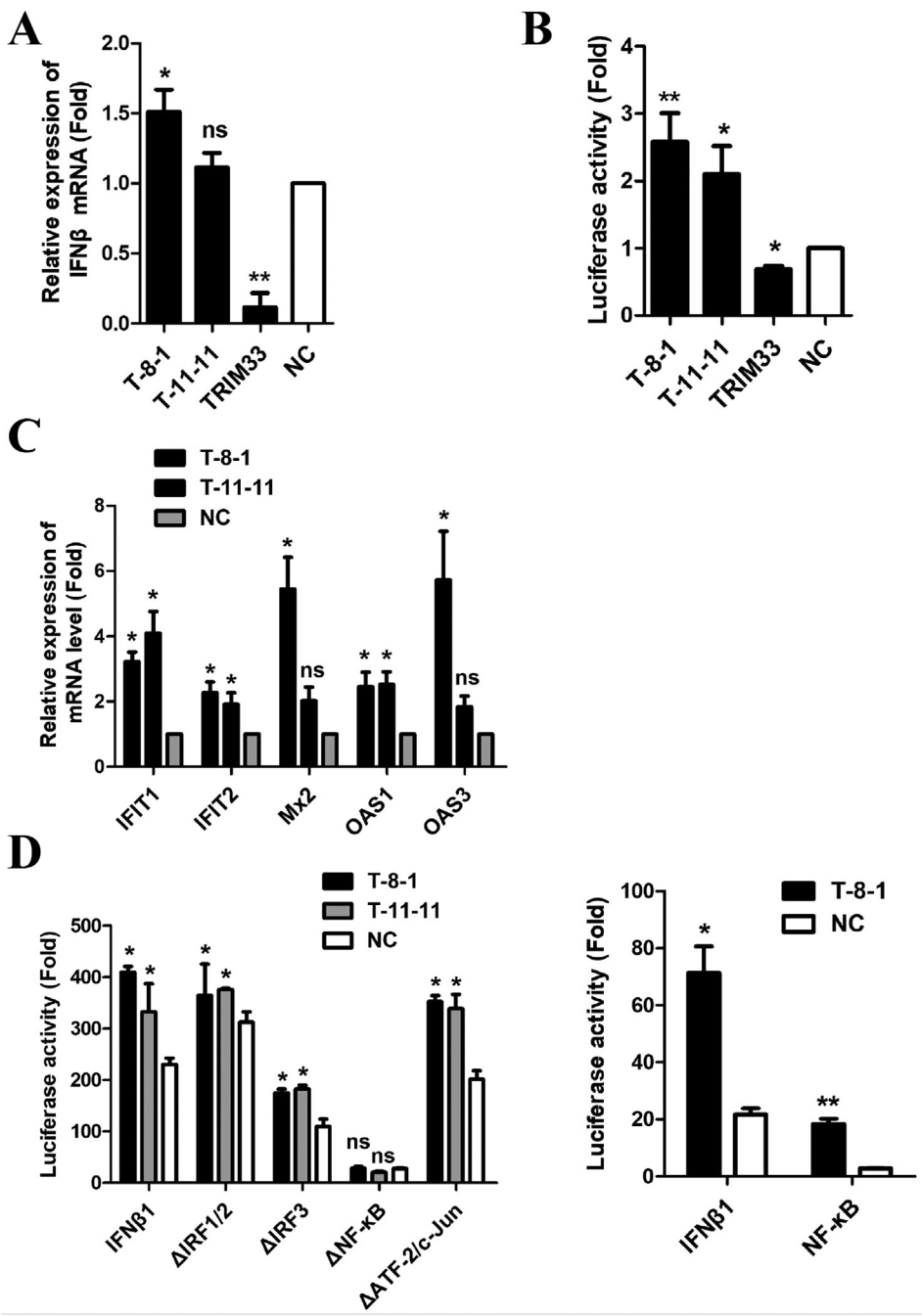

Fig. 8. TRIM33 inhibits IFNβ1 production and signaling primarily by affecting the NF-κB pathway. (A) IFNβ1 production was inhibited by TRIM33. *TRIM33*-knockout (T-8–1 and T-11–11), TRIM33-overexpressing and wild-type Marc145 cells were infected with CH-1a PRRSV for 36 h and then incubated with poly (I:C) (25 mg/mL) for 24 h. Cells were collected for qRT-PCR analysis of IFNβ1 production (normalized to GAPDH). (B) *IFNβ1* promoter vectors were cotransfected with pRL-TK into the three cell lines mentioned above for 36 h, followed by incubation with poly(I:C) (25 mg/mL) for 12 h. Then, the cells were harvested to assess luciferase activity. (C) IFNβ1 signaling was inhibited by TRIM33. qRT-PCR analysis of *IFIT1*, *IFIT2*, *MX2*, *OAS1*, and *OAS3* mRNA level (normalized to GADPH). (D) Several vectors carrying mutants of the *IFNβ1* promoter, including ΔIRFs, ΔNF-κB, ΔATF-2/c-Jun and NF-κB vectors, were cotransfected with pRL-TK into *TRIM33*-knockout cells (T-8–1 and T-11–11) and wild-type cells for 36 h, and the cells were then harvested to test luciferase activity. All data are representative of at least three independent experiments. The results are presented as the mean ± SEM (*$p < 0.05$, **$p < 0.01$, and ***$p < 0.001$); ns, not statistically significant.

Notably, the *piggyBac* transposon possesses readily detectable tags to probe the whole genome, including known genes and uncharacterized genes. In our study, in addition to the four genes mentioned above, other immune responses-related genes were also ranked in our gene list (Table S6), such as *CCR7*, *TNFSF4*, *TRIM27* and *STX4*, which have been reported to play important roles in the immune response or viral infection (Jindra et al., 2016; Ren et al., 2017; Wang et al., 2016; Zhang et al., 2017). Moreover, among the identified candidate genes, some genes have not been previously characterized, indicating that this forward genetic screening system effectively discovered novel genes, although the correlations between those uncharacterized genes and PRRSV resistance/susceptibility remain to be verified.

In addition, based on our findings that CDK17 and RNF168 inhibited PRRSV infection while TRIM33 promoted PRRSV infection, the modifications induced by the *piggyBac* system obviously exhibited powerful dual functions. For gain-of-function studies, strategies targeting only one allele of a gene in diploid cells may be sufficient for long-range transcriptional activation, ensuring wide genome coverage. With regard to loss-of-function studies, inactivation of only one gene copy will likely exert little effect on diploid cells, suggesting that some candidate genes might be missed in the final gene list.

As mentioned above, the Marc145 cell line was used in our screening system instead of a porcine cell line due to the lack of porcine cell types that can be widely applied under laboratory conditions. Indeed, many studies have attempted to express key receptors in non-permissive cells and support PRRSV replication (Calvert et al., 2007; Wang et al., 2013). However, all modified porcine cell lines have failed to act as replacements for Marc145 cells. Although modified 3D4/21 cells were used to validate the correlations between the candidate genes and PRRSV in our study, some defects still exist in PRRSV infection for this cell line. To some extent, the host factors identified in our system will contribute to the development of porcine cell lines permissive to

PRRSV infection. In addition, if porcine cell lines become available, the CRISPR/Cas9 system will also be utilized to screen genes essential for PRRSV resistance/susceptibility, which will further complement our current system.

Of note, to the best of our knowledge CDK17, RNF168, BCL2L15, and TRIM33 are all novel host factors involved in PRRSV infection. A previous study reported that inhibition of CDKs might prevent the efficient translation of IFNβ1, which would in turn prevent STAT activation and ISG expression (Oya Cingöza, 2018). Thus, we speculated that the depletion of CDK17 improved the proliferation of PRRSV in Marc145 cells and 3D4/21 cells potentially by inhibiting the translation of IFNβ1. It has also been reported that RNF168 plays a well-established role in DNA repair (Kizilors et al., 2017) and a critical role in regulating cell proliferation and survival, which may account for the anti-PRRSV effect of RNF168 on Marc145 cells and 3D4/21 cells, as mentioned above. The *BCL2L15* gene (also known as the BFK gene) is a proapoptotic member of the BCL2 family (Coultas et al., 2003). However, PRRSV has been reported to have anti-apoptotic activity during the initial phase of infection (Pujhari et al., 2016). Therefore, we speculated that BCL2L15 may inhibit PRRSV infection by promoting cell apoptosis. However, the precise mechanisms that underlie the interactions between these candidate genes and PRRSV need further validation.

TRIM33, together with TRIM24, TRIM28, and TRIM66, belongs to a TRIM subfamily whose members contain a plant homeodomain (PHD) and a bromodomain (BRD) in the C-terminal region (Herquel et al., 2011). Thus far, both TRIM24 and TRIM28 have been found to inhibit the IFN/STAT1 signaling pathway (Kamitani et al., 2008; Tisserand et al., 2011). It has been reported that TRIM33 deficiency alone cannot cause an IFN response in hepatocytes (Herquel et al., 2013). However, published evidence has shown that TRIM33 regulates *Ifnb1* enhanceosome loading and represses *Ifnb1* gene transcription shutdown during the late phase of macrophage activation (Ferri et al., 2015). Meanwhile, based on our results in Marc145 cells, we propose a potential model in which TRIM33 is upregulated following PRRSV infection and then leads to a decrease in NF-κB loading on the *Ifnb1* enhanceosome and the shutdown of *Ifnb1* transcription. Accordingly, TRIM33 could be regarded as a negative regulator of type I interferon production, which may be an immune evasion strategy of PRRSV.

In summary, the effects of CDK17, RNF168, BCL2L15, and TRIM33 on the different PRRSV strains tested in our study highlight the power and validity of our system to identify novel host factors involved in PRRSV infection. In addition, the discovery of host factors associated with PRRSV resistance/susceptibility can elucidate the mechanisms that underlies viral pathogenesis and host-pathogen interactions, which may be utilized in the future to prevent and control PRRS. Furthermore, the host factors discovered in this study will undergo in-depth study of their broad-spectrum effects on other viruses.

Overall, this study shows the value of performing *piggyBac* transposon screening to identify candidate genes associated with PRRSV infection. This method will not only help researchers prioritize genes for future studies to prevent and control PRRS but also provide more information about the system itself, which will contribute to its broader application in the future.

Acknowledgments

We would like to thank Prof. Guihong Zhang for providing XH-GD PRRSV and Prof. Hanchun Yang for providing the modified 3D4/21 cell line.

This work was supported by the National Major Program of Transgene (Grant number: 2016ZX08009-003-006).

Appendix A. Supporting information

Supplementary data associated with this article can be found in the online version at doi:10.1016/j.virol.2019.03.001.

References

Calvert, J.G., Slade, D.E., Shields, S.L., Jolie, R., Mannan, R.M., Ankenbauer, R.G., Welch, S.K.W., 2007. CD163 expression confers susceptibility to porcine reproductive and respiratory syndrome viruses. J. Virol. 81, 7371–7379.
Chen, L., Stuart, L., Ohsumi, T.K., Burgess, S., Varshney, G.K., Dastur, A., Borowsky, M., Benes, C., Lacy-Hulbert, A., Schmidt, E.V., 2013. Transposon activation mutagenesis as a screening tool for identifying resistance to cancer therapeutics. BMC Cancer 13, 93.
Chew, S.K., Rad, R., Futreal, P.A., Bradley, A., Liu, P., 2011. Genetic screens using the piggyBac transposon. Methods 53, 366–371.
Coultas, L., Pellegrini, M., Visvader, J.E., Lindeman, G.J., Chen, L., Adams, J.M., Huang, D.C., Strasser, A., 2003. Bfk: a novel weakly proapoptotic member of the Bcl-2 protein family with a BH3 and a BH2 region. Cell Death Differ. 10, 185–192.
Ding, S., Wu, X., Li, G., Han, M., Zhuang, Y., Xu, T., 2005. Efficient transposition of the piggyBac (PB) transposon in mammalian cells and mice. Cell 122, 473–483.
Ferri, F., Parcelier, A., Petit, V., Gallouet, A.S., Lewandowski, D., Dalloz, M., van den Heuvel, A., Kolovos, P., Soler, E., Squadrito, M.L., et al., 2015. TRIM33 switches off Ifnb1 gene transcription during the late phase of macrophage activation. Nat. Commun. 6, 8900.
Friedel, R.H., Friedel, C.C., Bonfert, T., Shi, R., Rad, R., Soriano, P., 2013. Clonal expansion analysis of transposon insertions by high-throughput sequencing identifies candidate cancer genes in a PiggyBac mutagenesis screen. PLoS One 8, e72338.
Guo, C., Chen, L., Mo, D., Chen, Y., Liu, X., 2015. DRACO inhibits porcine reproductive and respiratory syndrome virus replication in vitro. Arch. Virol.
Guo, G., Huang, Y., Humphreys, P., Wang, X., Smith, A., 2011. A PiggyBac-based recessive screening method to identify pluripotency regulators. PLoS One 6, e18189.
Han, J., Zhou, L., Ge, X., Guo, X., Yang, H., 2017. Pathogenesis and control of the Chinese highly pathogenic porcine reproductive and respiratory syndrome virus. Vet. Microbiol.
Hao, L., He, Q., Wang, Z., Craven, M., Newton, M.A., Ahlquist, P., 2013. Limited agreement of independent RNAi screens for virus-required host genes owes more to false-negative than false-positive factors. PLoS Comput. Biol. 9, e1003235.
Herquel, B., Ouararhni, K., Davidson, I., 2011. The TIF1alpha-related TRIM cofactors couple chromatin modifications to transcriptional regulation, signaling and tumor suppression. Transcription 2, 231–236.
Herquel, B., Ouararhni, K., Martianov, I., Le Gras, S., Ye, T., Keime, C., Lerouge, T., Jost, B., Cammas, F., Losson, R., et al., 2013. Trim24-repressed VL30 retrotransposons regulate gene expression by producing noncoding RNA. Nat. Struct. Mol. Biol. 20, 339–346.
Ivics, Z., Li, M.A., Mates, L., Boeke, J.D., Nagy, A., Bradley, A., Izsvak, Z., 2009. Transposon-mediated genome manipulation in vertebrates. Nat. Methods 6, 415–422.
Jindra, P.T., Conway, S.E., Ricklefs, S.M., Porcella, S.F., Anzick, S.L., Haagenson, M., Wang, T., Spellman, S., Milford, E., Kraft, P., et al., 2016. Analysis of a genetic polymorphism in the costimulatory molecule TNFSF4 with hematopoietic stem cell transplant outcomes. Biol. Blood Marrow Transplant. 22, 27–36.
Kamitani, S., Ohbayashi, N., Ikeda, O., Togi, S., Muromoto, R., Sekine, Y., Ohta, K., Ishiyama, H., Matsuda, T., 2008. KAP1 regulates type I interferon/STAT1-mediated IRF-1 gene expression. Biochem. Biophys. Res. Commun. 370, 366–370.
Kim, H.S., Kwang, J., Yoon, I.J., Joo, H.S., Frey, M.L., 1993. Enhanced replication of porcine reproductive and respiratory syndrome (PRRS) virus in a homogeneous subpopulation of MA-104 cell line. Arch. Virol. 133, 477–483.
Kim, H.S., Lee, K., Bae, S., Park, J., Lee, C.K., Kim, M., Kim, E., Kim, M., Kim, S., Kim, C., et al., 2017. CRISPR/Cas9-mediated gene knockout screens and target identification via whole-genome sequencing uncover host genes required for picornavirus infection. J. Biol. Chem. 292, 10664–10671.
Kizilors, A., Pickard, M.R., Schulte, C.E., Yacqub-Usman, K., McCarthy, N.J., Gan, S.U., Darling, D., Gaken, J., Williams, G.T., Farzaneh, F., 2017. Retroviral insertional mutagenesis implicates E3 ubiquitin ligase RNF168 in the control of cell proliferation and survival. Biosci. Rep.
Lunney, J.K., Chen, H.B., 2010. Genetic control of host resistance to porcine reproductive and respiratory syndrome virus (PRRSV) infection. Virus Res. 154, 161–169.
Oya Cingöza, baS.P.G., b.,c.,1, 2018. Cyclin-dependent kinase activity is required for type I interferon production. PNAS 115, E2950–E2959.
Petry, D.B., Holl, J.W., Weber, J.S., Doster, A.R., Osorio, F.A., Johnson, R.K., 2005. Biological responses to porcine respiratory and reproductive syndrome virus in pigs of two genetic populations. J. Anim. Sci. 83, 1494–1502.
Pujhari, S., Rasgon, J.L., Zakhartchouk, A.N., 2016. Anti-apoptosis in porcine respiratory and reproductive syndrome virus. Virulence 7, 610–611.
Rad, R., Rad, L., Wang, W., Cadinanos, J., Vassiliou, G., Rice, S., Campos, L.S., Yusa, K., Banerjee, R., Li, M.A., et al., 2010. PiggyBac transposon mutagenesis: a tool for cancer gene discovery in mice. Science 330, 1104–1107.
Ramage, H., Cherry, S., 2015. Virus-host interactions: from unbiased genetic screens to function. Annu. Rev. Virol. 2, 497–524.
Reiner, G., 2016. Genetic resistance - an alternative for controlling PRRS? Porc. Health Manag. 2, 27.
Ren, H., Elgner, F., Himmelsbach, K., Akhras, S., Jiang, B., Medvedev, R., Ploen, D., Hildt, E., 2017. Identification of syntaxin 4 as an essential factor for the hepatitis C virus life cycle. Eur. J. Cell Biol. 96, 542–552.
Rowland, R.R., Lunney, J., Dekkers, J., 2012. Control of porcine reproductive and respiratory syndrome (PRRS) through genetic improvements in disease resistance and tolerance. Front. Genet. 3, 260.
Thanawongnuwech, R., Suradhat, S., 2010. Taming PRRSV: revisiting the control strategies and vaccine design. Virus Res. 154, 133–140.
Tisserand, J., Khetchoumian, K., Thibault, C., Dembele, D., Chambon, P., Losson, R.,

2011. Tripartite motif 24 (Trim24/Tif1alpha) tumor suppressor protein is a novel negative regulator of interferon (IFN)/signal transducers and activators of transcription (STAT) signaling pathway acting through retinoic acid receptor alpha (Raralpha) inhibition. J. Biol. Chem. 286, 33369–33379.

Walden, R., Fritze, K., Hayashi, H., Miklashevichs, E., Harling, H., Schell, J., 1994. Activation tagging: a means of isolating genes implicated as playing a role in plant growth and development. Plant Mol. Biol. 26, 1521–1528.

Wang, D., Fang, L., Zhao, F., Luo, R., Chen, H., Xiao, S., 2011. Molecular cloning, expression and antiviral activity of porcine interleukin-29 (poIL-29). Dev. Comp. Immunol. 35, 378–384.

Wang, J., Teng, J.L., Zhao, D., Ge, P., Li, B., Woo, P.C., Liu, C.H., 2016. The ubiquitin ligase TRIM27 functions as a host restriction factor antagonized by Mycobacterium tuberculosis PtpA during mycobacterial infection. Sci. Rep. 6, 34827.

Wang, T., Birsoy, K., Hughes, N.W., Krupczak, K.M., Post, Y., Wei, J.J., Lander, E.S., Sabatini, D.M., 2015. Identification and characterization of essential genes in the human genome. Science 350, 1096–1101.

Wang, X., Wei, R., Li, Q., Liu, H., Huang, B., Gao, J., Mu, Y., Wang, C., Hsu, W.H., Hiscox, J.A., et al., 2013. PK-15 cells transfected with porcine CD163 by PiggyBac transposon system are susceptible to porcine reproductive and respiratory syndrome virus. J. Virol. Methods 193, 383–390.

Wu, S., Ying, G., Wu, Q., Capecchi, M.R., 2007. Toward simpler and faster genome-wide mutagenesis in mice. Nat. Genet. 39, 922–930.

Xue, H.Y., Ji, L.J., Gao, A.M., Liu, P., He, J.D., Lu, X.J., 2016. CRISPR-Cas9 for medical genetic screens: applications and future perspectives. J. Med. Genet. 53, 91–97.

YUSA, K., 2017. piggyBac Transposon. Microbiol Spectrum *3*, MDNA3-0028–2014.

Zhang, L., Ren, J., Shi, P., Lu, D., Zhao, C., Su, Y., Zhang, L., Huang, J., 2018. The immunological regulation roles of Porcine beta-1, 4 galactosyltransferase V (B4GALT5) in PRRSV infection. Front. Cell. Infect. Microbiol. 8, 48.

Zhang, L., Xiao, X., An, H., Wang, J., Ma, Y., Qian, Y.H., 2017. Inhibition of CCR7 promotes NF-kappaB-dependent apoptosis and suppresses epithelial-mesenchymal transition in non-small cell lung cancer. Oncol. Rep. 37, 2913–2919.

Zhang, Q., Huang, C., Yang, Q., Gao, L., Liu, H.C., Tang, J., Feng, W.H., 2016. MicroRNA-30c modulates type I IFN responses to facilitate porcine reproductive and respiratory syndrome virus infection by targeting JAK1. J. Immunol. 196, 2272–2282 (Baltim., MD: 1950).